

Buckling Models and Influencing Factors for Pipe Rehabilitation Design

Leslie K. Guice¹ and J.Y. Li²

Introduction

Structural design methodologies for pipeline rehabilitation systems are still in their infancy when compared to those components in bridges, buildings and other structures. Yet, design approaches for these older structural systems are continuously evolving and improving as more research is conducted and more experience is gained. The pipeline rehabilitation design process is also evolving as new research results are obtained, it is expected that enhancements in the design process will lead to more cost effective and durable designs. Tens of millions of feet of sewer pipelines have been rehabilitated with Cured-In-Place Plastic (CIPP) and Fold-and-Formed Plastic (FFP) pipe systems and some systems have proved that they can meet and exceed the performance requirements. However, with the tremendous needs faced by the U.S. in rehabilitating the underground infrastructure, it is imperative that future systems be designed as economically and with as high of quality as possible to serve the public for many years.

The purpose of this paper is to provide an overview of research which may be applicable to the structural design of CIPP and FFP pipes. Specifically, models which are related to the stability of flexible pipes formed inside stiff host pipes are considered and the effects of soil loading are not considered. The paper reviews literature about the basic theories for the buckling phenomenon of thin rings and cylinders under various loading forms, boundary conditions and failure configurations. It begins with the analysis of an unconstrained thin ring's buckling behavior, a relatively simple model but one which has been used widely for the design of CIPP liners. The paper also presents approaches for the buckling behavior of a thin ring rigidly encased within a confining enclosure ring. While long-term effects on the material behavior is known to be an important design parameter, it is not discussed in this paper. The theoretical approaches are compared with available experimental results.

Basic Buckling Theory of a Free Ring

The research on cylindrical tubes under external pressure dates from 1858 (Fairbairn: 1858). His experimental work concluded that the length of pipe and the ratio of diameter to wall thickness of the pipe were important parameters of the buckling pressure. Levy (1884) assumed the critical external pressure P_{cr} to be applied hydrostatically on a thin ring as buckling occurs and arrived at the following expression:

$$P_{cr} = \frac{3EI}{r^3} \quad (1)$$

¹ Professor and Head, Civil Engineering, Louisiana Tech University, Ruston, LA, 71272

² Research Assistant, Civil Engineering, Louisiana Tech University, Ruston, LA, 71272

where

P_{cr}	=	critical buckling pressure,
E	=	modulus of elasticity,
I	=	moment of inertia of the ring's cross-section,
r	=	mean radius of the ring.

G.H. Bryan (1888) analyzed an infinitely long pipe under external pressure through the minimum potential energy criterion of stability. This resulted in the following classical equation which assumes a plane strain condition. If the moment of inertia $I = t^3/12$, Equation 1 may be written as:

$$P_{cr} = \frac{2xE}{1-\nu^2} x \left(\frac{t}{D} \right)^3 \quad (2)$$

where

D	=	mean diameter of pipe,
t	=	mean pipe wall thickness,
ν	=	Poisson's ratio.

If Equation 2 is modified to include the dimension ratio DR , this equation can be written in the following form:

$$P_{cr} = \frac{2xE}{1-\nu^2} x \frac{1}{(DR-1)^3} \quad (3)$$

where

DR	=	Dimension Ratio, <i>outside pipe diameter/mean pipe wall thickness.</i>
------	---	---

The derivation of Equation 1 which is widely used as a basis for the design of underground pipes was summarized by Timoshenko in Theory of Elastic Stability (Timoshenko: 1961). This approach is based on the buckling phenomenon of a free (without outside constraint) thin curved bar with a circular axis under a uniform external pressure as illustrated in Figure 1. It is assumed that there exists a small deflection to make the ring slightly deflected from the circular form. With the geometrical relation shown in Figure 1, the bending moment at any cross-section of the ring can be expressed as:

$$M = M_0 - pr(w_0 - w) \quad (4)$$

where

M	=	bending moment,
M_0	=	bending moment at A and B,
p	=	external uniform pressure,
w	=	deflection of the ring in the radial direction,
w_0	=	deflection of the ring in the radial direction at A and B.

The deflection of the ring in radial direction w can be expressed by the following differential equation:

$$\frac{d^2w}{d\varnothing^2} + w = -\frac{Mr^2}{EI} \quad (5)$$

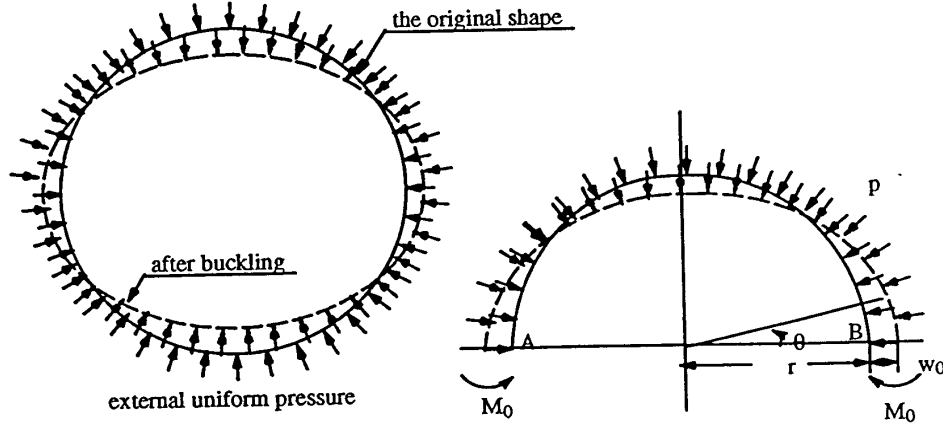


Figure 1 - The Buckling of a Free Ring

Defining k as:

$$k^2 = 1 + \frac{pr^3}{EI} \quad (6)$$

and substituting the expression for M from Equation 4, the differential equation becomes:

$$\frac{d^2w}{d\varnothing^2} + k^2w = \frac{-M_0r^2 + pr^3w_0}{EI} \quad (7)$$

The solution of this differential equation is expressed in the following general form:

$$w = A_1 \sin k\varnothing + A_2 \cos k\varnothing + \frac{-M_0r^2 + pr^3w_0}{EI + pr^3} \quad (8)$$

After applying boundary conditions, we obtain:

$$\sin \frac{k\pi}{2} = 0 \quad (9)$$

The smallest non-zero root of this equation is $k\pi/2=\pi$ and, therefore, $k = 2$. Substituting this into Equation 6 produces the minimum value of the critical pressure as follows:

$$P_{cr} = \frac{3EI}{r^3} \quad (10)$$

Higher roots of Equation 9 are $k=4, 6, 8\dots$, which indicate the higher modes of buckling (representing more waves). Higher critical buckling pressures correspond with the higher buckling modes and depend upon the type of boundary conditions imposed. Buckling will always follow the lowest mode without additional constraints. It should be noted that the first mode corresponds to rigid body motion and odd modes correspond to conditions wherein there is only one axis of symmetry. (See Figure 2.)

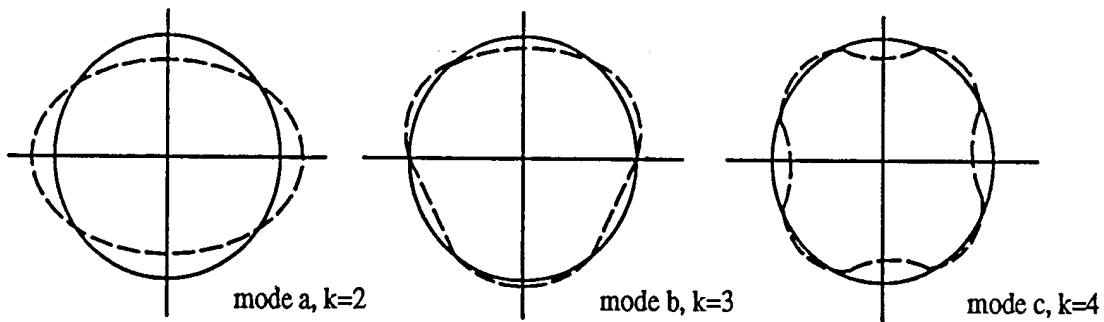


Figure 2 - Buckling Modes

Timoshenko presented other models which deserve consideration in the analysis of liners. From Figure 3, Timoshenko derived the equation for elastic buckling of a uniformly compressed circular arch. He obtained the following equation for the critical buckling pressure of a two-hinged inextensible arch with an arc subtended angle of 2α and with an inflection point at the center:

$$P_{cr} = \frac{EI}{r^3} \left(\frac{p^2}{a^2} - 1 \right) \quad (11)$$

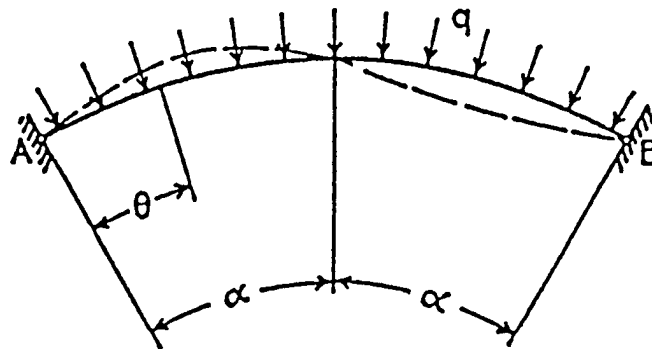


Figure 3 - Timoshenko's Uniformly Compressed Arch

As might be expected, this model yields the same results as Equation 10 when the angle $2\alpha = \pi$, since this condition represents exactly half of the model in Figure 1 between the two opposite inflection points. The model assumes that the initial center line of the arch to be a perfect circle, which can only occur if there is no bending moment present. However, bending moment is negligible as long as the applied pressure is small relative to the critical buckling pressure.

Timoshenko suggested a more general form to the equations he derived:

$$P_{cr} = g \frac{EI}{r^3} \quad (12)$$

and presented values of the coefficient Y for different arc angles and arch end conditions. Table 1 summarizes some of these values.

Table 1 - Timoshenko's Coefficient Y for Uniformly Compressed Circular Arches

2α (in degrees)	No hinges	One hinge	Two hinges
30	294	162	143
60	73.3	40.2	35
90	32.4	17.4	15
180	8.0	4.61	3.0

It should be noted from this work that the arc angle and end conditions can have an effect of at least two orders of magnitude on the critical buckling pressure, and the buckling pressure is increased as additional constraint is provided and as the subtended angle of the buckled portion of the arc decreases.

Buckling of a Thin Ring within a Rigid Cavity

Several approaches to the analysis of the failure of a thin ring encased in a rigid cavity of constant size can be found in the literature. In his study of steel tunnel linings, Amstutz (1969) presented a theory based on the assumption that failure occurs in the first mode when the yield stress in an outer fibre is first reached. Amstutz stated that under actual conditions, the plastic behavior of steel will cause the lining to yield at lower load than that needed to cause elastic snap-through buckling. However, for thin pipes, the primary mode of structural failure is buckling, which relates to the geometry of a structure and its stiffness, rather than the strength of the material.

Research on the buckling phenomenon of a thin ring within a rigid cavity began with the analysis of a confined complete ring subjected to a thermal expansion. This problem was analyzed by Lo, Bogdanoff, Goldberg, and Crawford (1962). They solved the

large-deflection equilibrium equation for the curved beam and defined the critical end-compressive (circumferential) load for the half-ring.

To extend this work to include the effect of an initial boundary imperfection, Hsu assumed a point obstacle at the bottom of a half-ring which created a vertical reaction when the end-compressive load P is applied (Hsu: 1964). Hsu developed the nonlinear differential equation of equilibrium of the segment at which buckling occurs. Applying boundary conditions and integrating this differential equation, the solution is expressed in terms of elliptic functions and the relation between the end compressive load and the total end displacement is obtained. This problem is significant for the failure analysis of CIPP liners because the point obstacle could be considered as a defect existing in the pipe prior to rehabilitation.

Zagustin investigated a thin, elastic ring constrained in a rigid circular surface under a uniformly distributed parallel loading (Zagustin: 1967). An analytical solution for the relation between the load and the associated deformed shape of the ring was found.

While this work contributes to the understanding of constrained pipe behavior, the resulting models are not particularly applicable to the current problem. Other constrained models which are more relevant are summarized below.

Chicurel's Model

R. Chicurel (1968) considered “*shrink buckling*” of a thin elastic circular ring which is compressed by being inserted into a circular opening of smaller diameter than the outside diameter of the free ring. The shrink buckling phenomenon is not the same as the buckling phenomenon of CIPP liners because shrink buckling is caused only by hoop compression, while the buckling of CIPP liners is due to external uniform pressure. For shrink buckling, the hoop compressive force is relieved immediately after buckling occurs. For a pipe under hydrostatic pressure, the load is sustained after buckling is initiated and the energy associated with the sustained pressure must be considered. Nevertheless, the approaches for shrink buckling and external uniform pressure are comparable with each other up until the point where buckling is initiated.

Figures 4 & 5 illustrate the shrink buckling model of a thin ring and the diagram of the deformed geometry in the portion of the ring presented by Chicurel. He used the following equation, taken from Timoshenko (1961) for the deflection of an axially compressed curved beam, to describe the buckled configuration shown in Figure 5:

$$w = \frac{2a}{n^2} x \left[\frac{\cos\left(1 - \frac{2x}{l}\right)}{\cos(n)} - 1 \right] \quad (13)$$

where

w	=	distance from axis of buckled arc to x-axis,
Φ	=	one-half of central angle subtended by buckled arc
v^2	=	$(Pl)/(4EI)$,
l	=	chordal length of buckled arc,
x	=	coordinate along chord of buckled portion of ring,

Combining the geometry of deformations, boundary conditions of the stability equation, and the assumption of no-friction existing between the ring and outside constraint, the equation for the prebuckling hoop compressive force P_0 which causes the thin ring to buckle is:

$$P_0 = 0.061AE\alpha^3 \quad (14)$$

where

P_0	=	prebuckling hoop compressive force,
A	=	cross-sectional area of ring,
α	=	$3.54 (l/Ar^2)^{1/5}$, one half of central angle subtended by buckle arc.

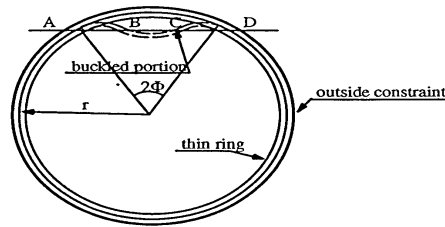


Figure 4 - Chicurel's Shrink Buckling Model of a Thin Ring

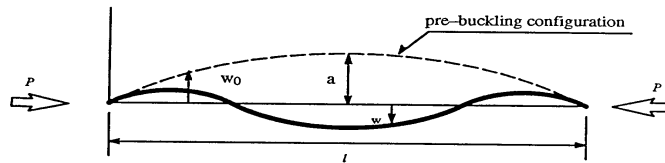


Figure 5 - Chicurel's Geometry of Deformation

Combining expressions of P_0 and α yields:

$$P_0 = 2.67AE\alpha \left(\frac{l}{Ar^2} \right)^{3/5} \quad (15)$$

Similar results can be developed for the critical pressure of a thin tube under external uniform pressure. If a thin ring is compressed by an external uniform pressure P , the relation between the hoop compression P_0 and the uniform external pressure could be

related by $P = P_0/r$. Then substituting the moment of inertia for the cross-section of a thin ring, and considering the effect of Poisson's ratio for the plane strain condition of an infinitely long pipe, the equivalent critical buckling pressure of a rigidly encased thin pipe as determined from the analysis of shrink buckling follows:

$$P_{cr} = \frac{2.76xE}{1-\nu^2} \left(\frac{t}{D} \right)^{\frac{11}{5}} \quad (16)$$

It should be noted again that Equation 16 was derived from the shrink buckling of a thin ring which neglects the effects of applied pressures which occur over the arc after buckling is initiated. Also, the critical pressure P_{cr} was equivalently transformed from the hoop compression P_0 .

Cheney's Model

Cheney (1971) used small deflection, linear theory in considering the buckling of rigidly encased rings or shells under an external uniform pressure. He further assumed that the walls of the cavity move inward with the ring resisting outward movement but not inward movement, and he included extensional deformations of the ring. The principle of minimum potential energy was used to derive the equations of equilibrium governing the buckling of a circular ring. The energy expression is obtained by summing the internal strain energy due to extension and bending of the centroidal axis minus the work done by the external pressure and boundary forces and moments:

$$V = \frac{1}{2} \int \left\{ EA\epsilon_0^2 + EI\kappa^2 - \frac{P_{cr}}{r} [(u')^2 - u^2] \right\} r d\mathbf{q} \quad (18)$$

$$- \left[N_z w + N_x u + \frac{M}{r} (w + u) \right]_{\Phi_1}^{\Phi_2}$$

where	V	=	potential energy,
	A	=	cross-sectional area of ring,
	N_z	=	shear stress resultant
	N_x	=	hoop stress resultant
	u	=	radial deflection (positive inward),
	w	=	curvilinear displacement along z axis
	θ	=	curvilinear coordinate along z axis, $0=z/R$
	M	=	bending moment in cross-section,
	Φ_1, Φ_2	=	values of θ at the boundaries and
	K	=	$(u'' + u)/r^2$
	ϵ_0	=	$(w' - u)/r$

By minimizing the potential energy and by successively integrating the parts, Cheney derived the following differential equations governing buckling of the ring:

$$\frac{EA}{r^2}(w' - u) = Ck^2 \frac{EI}{r^4} \quad (19)$$

$$u'' + (1 + k^2)u'' + k^2 = Ck^2 \quad (20)$$

where k is defined as follows

$$k^2 = \frac{Pr^3}{EI} + 1 \quad (21)$$

If the boundaries of the buckling portion are confined at $\theta = \Phi_1 = -\Phi$ and $\theta = \Phi_2 = +\Phi$ and the appropriate boundary conditions are applied to the differential equations, the value of k can be determined by the following equation:

$$k = \frac{r}{r} \left(\frac{1 - \Phi \cot \Phi}{p \cot \Phi} \right)^{1/2} \quad (22)$$

where $r = (I / A)^{1/2} = (t^3 / 12t)^{1/2} = 0.289t$

and, as the critical arc angle Φ goes to zero:

$$k = \frac{r\Phi^{3/2}}{r\sqrt{3p}} \quad (23)$$

Cheney used a graphical solution to show that the minimum value of $k_{cr} = 3.0$ for the case of $r/p=0$ and

$$k = 157 \left(\frac{r}{r} \right)^{2/5} = 2.58 \left(\frac{r}{t} \right)^{2/5} \quad (24)$$

for $r/p \rightarrow \infty$.

The critical pressure P_{cr} of the rigidly encased thin ring is determined by rewriting Equation 21:

$$P_{cr} = \frac{(k^{2-1})EI}{r^3} \quad (25)$$

For relatively thin pipes (e.g., $DR > 30$, and $r/t > 15$). $k^2 - 1 \cong k^2$. Substituting Equation 24 into Equation 25, and considering an infinitely long pipe, then leads to the following equation:

$$P_{cr} = 2.55xEx \left(\frac{t}{D} \right)^{\frac{11}{5}} \quad (26)$$

Glock's Approach

Glock (1977) analyzed the stability problem of a rigidly encased thin ring under external hydrostatic pressures as well as under thermal load. Figure 6 shows the model of the rigidly encased thin ring under external uniform pressure. Glock's model assumes that there is no friction between the ring and the rigid cavity, but unlike Cheney and Chicurel's models, Glock's model does not require the cavity wall to move inward with the ring. Glock used nonlinear deformation theory to develop his model. According to the Glock's approach, the deflection is described by the following equation:

$$w = w_1 \sin^2 \frac{pq}{2f} \quad (27)$$

where

w	=	deflection of the buckled area of the thin ring,
w_1	=	deflection amplitude in the buckled area of the thin ring,
θ	=	variable of angle,
Φ	=	open angle within the buckled area of the thin ring.

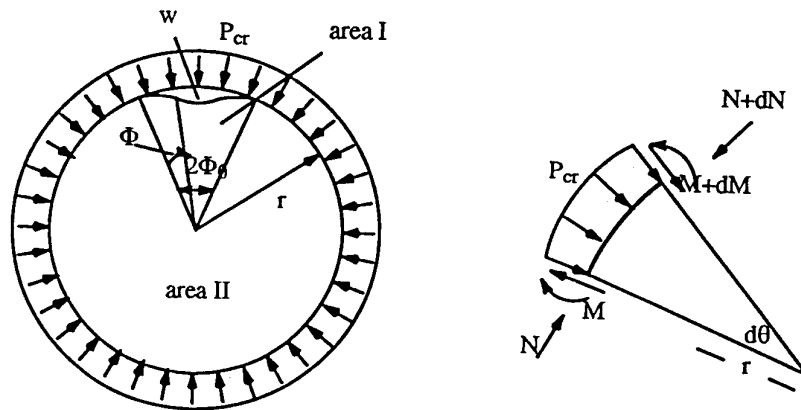


Figure 6 - Glock's Constrained Ring Model

As the ring buckles, the potential energy includes three parts: (1) the flexural moment M within the buckling region (area I in Figure 6), (2) the hoop compressive force N , and (3) the external uniform pressure P_{cr} accumulated during the buckling process. This last part of the potential energy was not taken into account in the model of shrink buckling. Combining these three parts of potential energy Π , the following expression can be obtained:

$$\Pi = \frac{1}{2} \cdot \frac{EI}{r^3} \int_0^{\Phi_0} (w + \dot{w})^2 dq + \int_0^{\Phi_0} \frac{N^2}{2EF} r dq - \int_0^{\Phi_0} P_{cr} w r dq \quad (28)$$

where

Π	=	potential energy,
EI	=	flexural stiffness of the thin ring,

EF = tensile stiffness of the thin ring,
 N = hoop compressive force.

After making substitutions and integrating Equation 28, the potential energy may be written:

$$\Pi = \frac{1}{16} \frac{EI}{r^3} \left(\frac{p}{\Phi} \right)^4 w_1^4 \Phi = + \frac{N^2}{2} \cdot \frac{rp}{EF} - \frac{P_{cr} r}{2} w_1 \Phi \quad (29)$$

The minimum potential energy criterion should satisfy the requirement:

$$d\Pi = \frac{\partial \Pi}{\partial w_1} dw_1 + \frac{\partial \Pi}{\partial q} dq = 0 \quad (30)$$

which leads to the following differential equations:

$$\frac{\partial \Pi}{\partial w_1} = \frac{1}{8} \cdot \frac{EI}{r^3} \Phi \left(\frac{p}{\Phi} \right)^4 w_1 + N \frac{\partial N}{\partial w_1} \cdot \frac{rp}{EF} - P_{cr} \frac{r\Phi}{2} = 0 \quad (31)$$

$$\frac{\partial \Pi}{\partial q} = -\frac{3}{16} \cdot \frac{EI}{r^3} \left(\frac{p}{\Phi} \right)^4 w_1^2 + N \frac{\partial N}{\partial \Phi} \frac{rp}{EF} - P_{cr} \frac{Rw_1}{2} = 0 \quad (32)$$

Solving Equations 31 and 32 simultaneously yields the following equation in determining the dimensionless value for the critical hydrostatic pressure of the rigidly encased thin ring:

$$\left(\frac{P_{cr} r^3}{EI} \right)_{cr} = \alpha_{cr} = 0.969 \left(\frac{EFr^2}{EI} \right)^{2/5} \quad (33)$$

where α_{cr} = critical load parameter.

Equation 33 is the result of Glock's approach for predicting the critical pressure of a rigidly encased thin ring under an external uniform pressure. If the assumption is made that the flexural modulus of elasticity is approximately equal to the tensile modulus, and considering the condition of plane-strain, Equation 33 can be simplified as follows:

$$P_{cr} = \frac{1.0xE}{1-n^2} \left(\frac{t}{D} \right)^{2.2} \quad (34)$$

Discussion of Models

The models reviewed above all result in equations for the critical buckling pressure which are similar in form. The basic form of these equations is:

$$P_{cr} = \frac{Cx E}{1 - \nu^2} \frac{1}{(DR - 1)^b} \quad (35)$$

where C = coefficient
 b = exponent

The resulting coefficients and exponents for each model are summarized in Table 2.

Table 2 Buckling Equation Parameters

MODEL	Coefficient, C	Exponent, b
Timoshenko unconstrained	2.0	3.0
Timoshenko compressed arch	2.0→	3.0
Chicurel shrink buckling	2.76	2.2
Cheney encased ring	2.55	2.2
Glock encased ring	1.0	2.2

It should be noted that there are consistencies in the exponents for the different models. Those models which impose a constraint around the surface tend to yield solutions with an exponent of 2.2. The coefficients of the last three models can vary significantly depending upon the types of assumptions made. Each of the models presented has merits and under certain conditions might be the most appropriate one for consideration. However, each of the models also has limitations, and even for the most complex of the models some factors have not been included.

The stability analysis of restrained pipe is complicated by nonlinear geometries, various interface and boundary conditions, and nonlinear material behavior. Other factors which must ultimately be considered by a model include visco-elastic effects, host pipe geometry (such as ovality) and defects as well as other anomalies which may occur. The size of the gap between a liner and its host pipe will affect the buckling resistance since the gap size influences the boundary conditions.

Evaluation of Equations Through Experimental Results

The application of any analytical model into practice requires the validation and calibration through experimental research. Until analytical models have been developed to include the necessary conditions, the resulting equations must be tuned by experiment and safety factors must be included to address various uncertainties.

The equations derived by the approaches presented above may be evaluated through comparisons with available experimental data. The mathematical tools of linear

regression and error analysis may be employed to develop the value of the coefficient and exponent based on the experimental results.

Very little CIPP pipe experimental data exists for evaluating the theoretical models. Some organizations are known to have conducted proprietary experimental work related to this study, but most have not yet been published in the public domain. Three sets of data which are used in this paper include work done by Aggarwal and Cooper at Coventry Polytechnic (1984), Watkins at Utah State University (Lo, et. al, 1993), and Guice and others at Louisiana Tech University (1994)

Aggarwal and Cooper's Tests

Aggarwal and Cooper conducted external pressure tests of Insituform liners. In these tests the liners were inserted in steel pipes. Then the pressure was employed and increased between the liner and casing in increments of approximately 1/10th of the expected failure pressure, until failure. Internal observation was carried out to determine when bulging occurred. The experimental failure pressure was found to be much larger than the theoretical buckling pressure obtained by Equation 3.

An “*enhancement factor*” was defined by Aggarwal and Cooper’s as $K = P_{\text{test}}/P_{\text{theory}}$. The enhancement factor reflects the difference between the results by experiment and theory. Aggarwal and Cooper indicated that the values of the enhancement factor varied from 6.5 to 25.8 with a range of pipe DRs from approximately 30 to 90. Aggarwal and Cooper indicated that 46 of the 49 tests gave a value of *K* greater than 7. The term “enhancement” was used because the buckling resistance of the liners appeared to be significantly enhanced by the constraining effects of the host pipe. For the remaining portion of this paper, *K* will simply be referred to as a factor which compensates for the deviation between experimental results and theory.

Aggarwal and Cooper’s tests are selected for the purposes of comparison and verification of the proposed analytical models because they represent the most comprehensive experimental results currently known to exist, including (1) a relatively large sample (49 specimens); (2) a relatively large range of standard dimension ratios (from 29.86 to 90.25); and (3) a variety of material properties (modulus of elasticity from 130,000 psi to 366,000 psi).

Shell Development Company Tests

Shell Development Company conducted an experimental program at Utah State University to evaluate the collapse resistance of CIPP liners made with various epoxy resins (Lo, Chang, Zhang, and Wright: 1993). The specimens of the tests had a constant outside diameter and different thicknesses. The results of these tests were also analyzed to determine the enhancement factor *K*. Lo found the values of the factors ranged from 9.66 to 15.1.

Louisiana Tech University's Tests

Louisiana Tech University is currently conducting research on the long-term effects of hydrostatic pressures on CIPP and FPP liners under the Corps of Engineers Construction Productivity Advancement Research (CPAR) program (Guice and Norris: 1993). Seven different products from five companies are being evaluated. Several short-term tests for each product have been completed. Test specimens are 12 inches in diameter and DRs range from 30 to 60. Complete test results for this test program will be published later this year.

Analysis of Data

If the term P_{test} is defined as the experimental buckling pressure and the factor K is defined as the ratio of P_{test} to P_{cr} , the following equation can be obtained:

$$P_{test} = KxP_{cr} = \left[\frac{Cx E}{1 - \nu^2} x \frac{1}{(DR - 1)^b} \right] x K \quad (36)$$

and

$$\text{Log} \left(\frac{P_{test}}{E / (1 - \nu^2)} \right) = \text{Log} C - b \text{Log} (DR - 1) + \text{Log} K \quad (37)$$

If the subscript of i is used to designate individual test results ($i = 1, 2, 3, \dots, n$), where n is the number of the tests in the sample, Equation 37 can be expressed in terms of subscript i as follows:

$$\text{Log} \left(\frac{P_{test,i}}{E_i / (1 - \nu^2)} \right) = \text{Log} C - b \text{Log} (DR_i - 1) + \text{Log} K_i \quad (38)$$

The values of C and b may be determined by the particular analytical equation used for the critical pressure P_{cr} . $P_{test,i}$ is the test result of i th specimen, while E_i and DR_i are the corresponding material and geometric properties. Substituting the notation of Y_i and X_i into Equation 38 yields:

$$Y_i = a - bX_i + e_i \quad (39)$$

The error ε_i reflects the deviation between the theoretical and experimental buckling pressures of a specific test specimen. If the results of a series of short-term buckling tests are employed to verify a theoretical equation with corresponding values of constant a ($\text{Log} C$) and b , a sample ε_i ($i=1, 2, \dots, n$) can be obtained and the mean \bar{e} and standard deviation s of the test sample can be determined. The error \bar{e} , and its corresponding factor K , are affected by many known and unknown factors of the specimen and the process of testing. Usually, the random variable ε can be approximately assumed to follow a normal distribution.

When evaluating different equations, the theoretical formula is first selected and the error related to the deviation between the theoretical and experimental buckling pressures is determined. On the other hand, it would be interesting to determine the coefficients and exponents which could best predict the buckling pressures. To do this, “best-fitting” regression may be employed.

The objective for determining a best-fitting regression Y_e is to minimize the errors $\epsilon_i (i=1,2,3,\dots,N)$. As illustrated in Figure 7, some data points deviate more from the regression line than others. However, if the regression line is adjusted to reduce the larger deviations, it will result in increasing other deviations. Some data points are positive, since Y_e is less than Y , while the deviations for other data points are negative, since Y_e is larger than Y . The method generally used to obtain a best-fitting regression line is the method of least squares. This method produces a regression line which

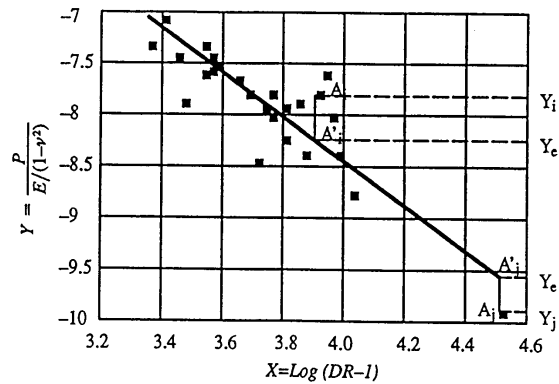


Figure 7 - Regression Line

reduces the sum of the squared deviations (errors) of observed Y values from the regression line to a minimum. A fundamental property of the least squares regression line is that the sum of the errors computed is equal to zero.

Results

If the coefficients and exponents presented in Table 2 are substituted into Equation 38, the data may be analyzed to yield estimates of the mean error \bar{e} and factor corresponding with the error $K\bar{e}$ for each theoretical equation. The results of this analysis for Timoshenko’s unconstrained model and Glock’s constrained model are presented in Table 3. The results of the best-fitting regression analysis of Aggarwal and Cooper’s data are also presented in Table 3.

Table 3 - Evaluation of Analytical Models With Aggarwal and Cooper Data

Equation	C	b	\bar{e}	$K\bar{e}$	s
Timoshenko	2.0	3.0	1.075	11.89	0.139
Glock	1.0	2.2	0.078	1.20	0.107
Best Fitting Regression	1.07	2.17	0.0	1.0	0.107

Since the other analytical models presented are similar in form and vary only by a constant with either Timoshenko's or Glock's equations, the results for the other models were not included for comparison in Table 3. It should be noted that the average deviations between the theoretical and experimental buckling pressures are smaller for Glock's equation than Timoshenko's equation. Further, a best-fitting regression analysis results in coefficients and exponents very similar to those for Glock's model.

The test results from Shell Development Company and Louisiana Tech university were analyzed for comparison with the Timoshenko and Glock equations. The data were analyzed to determine average values of statistical deviations based upon each of the two models. Those results are summarized in Table 4. The smaller deviations between experiment and theory are again noted for Glock's equation:

Table 4 - Analysis of Data

Data	Timoshenko			Glock		
	\bar{e}	$K\bar{e}$	s	\bar{e}	$K\bar{e}$	s
Aggarwal and Cooper	1.075	11.89	0.139	0.078	1.20	0.107
Shell Development	1.126	13.38	0.057	0.043	1.104	0.056
Louisiana Tech University	0.992	9.81	0.109	-0.046	0.900	0.076

Conclusions

The development of several analytical models for CIPP and FPP have been presented and compared with experimental data. On a preliminary basis, it would appear that the coefficient and exponent suggested by Glock's model may be the most appropriate values for use in conjunction with the experimental results obtained to date. However, the analysis and results presented in this paper are not intended to be complete, and additional research is required before any new equations can be recommended as a design expression.

References

Aggarwal, S. C., and Cooper, M. J. (1984). "External Pressure Testing of Insituform Linings." Internal Report, Coventry (Lanchester) Polytechnic.

Amstutz, E. Das Einbeulen von Schaecht - und Stollenpanzerungen. (1969). *Schweizerische Bauzeitung*. Vol. 87, pp. 541 - 549. (English Translation: United States Department of the Interior, Bureau of Reclamation, Translation No. 825, 1969).

Bryan, G.H. (1888). "Application of the Energy Test to the Collapse of a Long Pipe Under External Pressure." *Proceedings of the Cambridge Philosophical Society*, Vol. 6, 287-292.

Cheney, J.A. (1971). "Pressure Buckling of Ring Encased in Cavity." *Journal of Engineering Mechanics*, ASCE, 333 - 343.

Chicurel, R. (1968). "Shrink Buckling of Thin Circular Rings." *Journal of Applied Mechanics*, ASME, 608 - 610.

Fairbairn, W. (1858). "On the Resistance of Tubes to Collapse." *Philosophical Transactions of the Royal Society*, Vol. 148, pp 389 - 413.

Guice, L. K. and Norris, C. (1993) "Long-Term Hydrostatic Pressure Testing of Liner Materials." Proceedings of Trenchless Technology, An Advanced Technical Seminar. Vicksburg, Ms.

Hsu, P. T., Elkon, J. and Pian, T. H. H. (1964) "Note on the Instability of Circular Rings Confined to a Rigid Boundary." *Journal of Applied Mechanics*, Vol. 31. No. 3, Trans. ASME, Series E, Vol. 86, 559 - 562.

Levy, M. (1884). "Me'memoire sur un nouveau cas inte'grable du proble'm de l'elastique et l'une de ses applications" [Memoir on a new integrable case of the problem of elasticity and one of its applications]. *J. Math Pure et Appl. (Liouville)*, Series 3, Vol. 10, pp 5-42.

Lo, Hsu, et al. (1962). "A Buckling Problem of a Circular Ring." *Proceedings of the Fourth U.S. National Congress of Applied Mechanics*, ASME, 691 - 695.

Lo K.H., Chang, B.T.A. Zhang, Q. and Wright, W.J. (1993). "Collapse Resistance of Cured-In-Place Pipes." Proceedings of the North American No-Dig '93., NASTT, San Jose, CA.

Timoshenko, S.P., and Gere, J.M. (1961) *Theory of Elastic Stability*, 2nd ed., McGraw-Hill, New York.

Zagustin, E.A., and Herrmann, G. (1967). "Stability of an Elastic Ring in a Rigid Cavity." *Journal of Applied Mechanics*, Vol. 34, No. 2, Trans., ASME, Series E. Vol. 89, 263-270.